Available online at www.sciencedirect.com
ScienceDirect
Engineering Structures 29 (2007) 305–316
ENGINEERING STRUCTURES
www.elsevier.com/locate/engstruct

Assessment of current nonlinear static procedures for seismic evaluation of buildings

Erol Kalkan, Sashi K. Kunnath*

Department of Civil and Environmental Engineering, University of California, Davis, CA 95616, United States

Received 9 September 2005; received in revised form 7 April 2006; accepted 27 April 2006
Available online 27 June 2006

Abstract

An essential and critical component of evolving performance-based design methodologies is the accurate estimation of seismic demand parameters. Nonlinear static procedures (NSPs) are now widely used in engineering practice to predict seismic demands in building structures. While seismic demands using NSPs can be computed directly from a site-specific hazard spectrum, nonlinear time-history (NTH) analyses require an ensemble of ground motions and an associated probabilistic assessment to account for aleatoric variability in earthquake recordings. Despite this advantage, simplified versions of NSP based on invariant load patterns such as those recommended in ATC-40 and FEMA-356 have well-documented limitations in terms of their inability to account for higher mode effects and the modal variations resulting from inelastic behavior. Consequently, a number of enhanced pushover procedures that overcome many of these drawbacks have also been proposed. This paper investigates the effectiveness of several NSPs in predicting the salient response characteristics of typical steel and reinforced concrete (RC) buildings through comparison with benchmark responses obtained from a comprehensive set of NTH analyses. More importantly, to consider diverse ground motion characteristics, an array of time-series from ordinary far-fault records to near-fault motions having fling and forward directivity effects was employed. Results from the analytical study indicate that the Adaptive Modal Combination procedure predicted peak response measures such as inter-story drift and component plastic rotations more consistently than the other NSPs investigated in the study.
© 2006 Elsevier Ltd. All rights reserved.

Keywords: Adaptive pushover; Nonlinear static analysis; Near-fault records; Seismic evaluation

1. Introduction

In performance assessment and design verification of building structures, approximate nonlinear static procedures (NSPs) are becoming commonplace in engineering practice to estimate seismic demands. In fact, some seismic codes have begun to include them to aid in performance assessment of structural systems (e.g., Eurocode 8 [1]; Japanese Design Code [2]). Although seismic demands are best estimated using nonlinear time-history (NTH) analyses, NSPs are frequently used in ordinary engineering applications to avoid the intrinsic complexity and additional computational effort required by the former. As a result, simplified NSPs recommended in ATC-40 [3] and FEMA-356 [4] have become popular. These procedures are based on monotonically increasing predefined load patterns until some target displacement is achieved. However, it is now well-known that these simplified procedures based on invariant load patterns are inadequate to predict inelastic seismic demands in buildings when modes higher than first mode contribute to the response and inelastic effects alter the height-wise distribution of inertia forces (e.g., Gupta and Kunnath [5]; Kunnath and Kalkan [6]; Kalkan and Kunnath [7]; Goel and Chopra [8]). In order to overcome some of these drawbacks, a number of enhanced procedures considering different loading vectors (derived from mode shapes) were proposed. These procedures attempt to account for higher mode effects and use elastic modal combination rules while still utilizing invariant load vectors. The modal pushover analysis (MPA) of Chopra and Goel [9], modified modal pushover analysis (MMPA) of Chopra et al. [10], and the upper-bound pushover analysis (UBPA) procedure of Jan et al. [11] are examples of this approach.

Another class of enhanced pushover methods is the adaptive pushover procedures, where the load vectors are progressively

* Corresponding author. Tel.: +1 530 754 6428; fax: +1 530 752 4833.
E-mail address: skkunnath@ucdavis.edu (S.K. Kunnath).

0141-0296/$ - see front matter © 2006 Elsevier Ltd. All rights reserved.
doi:10.1016/j.engstruct.2006.04.012

updated to consider the change in system modal attributes during inelastic phase. Gupta and Kunnath [5] proposed an adaptive algorithm utilizing an elastic demand spectrum. In this procedure, equivalent seismic loads are calculated at each pushover step using the instantaneous mode shapes. The corresponding elastic spectral accelerations are used for scaling of the lateral loads which are applied to the structure in each mode independently. Several other force-based or displacement based pushover procedures utilizing adaptive load patterns have also been proposed (e.g., Elnashai [12]; Antoniou and Pinho [13]). More recently, a new adaptive modal combination (AMC) procedure, whereby a set of adaptive mode-shape based inertia force patterns is applied to the structure, has been developed (Kalkan and Kunnath [14]). The methodology has been validated for regular moment frame buildings.

With the increase in the number of alternative pushover procedures proposed in recent years, it is useful to identify the potential limitations of these methods and compare and contrast their effectiveness in simulating seismic demands at the structure, story and component level. In this paper, the ability of enhanced nonlinear static procedures to simulate seismic demands in a set of existing steel and reinforced concrete (RC) buildings is explored through comparisons with benchmark results obtained from a comprehensive set of NTH analyses considering ground motions having diverse characteristics. The earthquake recordings were carefully compiled so as to reflect characteristics of normal far-fault records and typical near-fault records having forward-directivity and fling effects.

2. Review of major nonlinear static procedures

NSPs can be classified into three major groups based on the type of lateral load patterns applied to the structural model during the analysis: invariant single load vectors (FEMA-356); invariant multi-mode vectors (MMPA and UBPA); and adaptive load vectors (AMC). In this section, a brief overview of these typical methodologies is presented.

2.1. FEMA-356 lateral load patterns

Currently, two sets of lateral load distributions are recommended in FEMA-356 for nonlinear static analysis. The first set consists of a vertical distribution proportional to (a) pseudo lateral load (this pattern becomes an inverted triangle for systems with fundamental period $T_1 < 0.5$ s); (b) elastic first mode shape; (c) story shear distribution computed via response spectrum analysis. The second set encompasses mass proportional uniform load pattern and adaptive load patterns (though the FEMA document refers to an adaptive pattern, a detailed procedure is not provided). FEMA-356 recommends that at least one load pattern from each set be used to obtain the response envelope. Therefore, in this study, the most commonly used load distributions, viz., a load vector proportional to the first mode shape and a load vector proportional to the story mass, are employed. The results presented in this paper represent the envelope of the two distributions.

2.2. Modified modal pushover analysis (MMPA)

The modified modal pushover analysis (MMPA), which has been recently developed by Chopra et al. [10] is an extension of modal pushover analysis (MPA), combines the elastic influence of higher modes with the inelastic response of a first mode pushover analysis using modal combination rules (such as SRSS). The procedure involves conducting a nonlinear response history analysis (NRHA) of the first-mode SDOF system unless an inelastic response spectrum is available for the target (design) ground motion. Details of the implementation are described in Chopra et al. [10].

2.3. Upper-bound pushover analysis (UBPA)

Unlike the MMPA where the response is obtained from the combination of individual analyses using different mode shapes, the upper-bound pushover analysis (UBPA) proposed by Jan et al. [11] is based on utilizing a singe load vector obtained as the combination of the first mode shape and a factored second mode shape. The spectral displacements (D_n) corresponding to elastic first and second mode periods are estimated from the elastic spectrum of the considered ground motion and the upper-bound contribution of the second mode is established using modal participation factors (Γ_n), as follows:

$$(q_2/q_1) = |(\Gamma_2 D_2)/(\Gamma_1 D_1)|. \tag{1}$$

The invariant load vector (F) is then computed as the combination of first and second mode shapes:

$$F = w_1^2 m\phi_1 + w_2^2 m\phi_2(q_2/q_1). \tag{2}$$

2.4. Adaptive modal combination (AMC) procedure

The AMC procedure was developed to integrate the essential concepts of the following three methods: the capacity spectrum method recommended in ATC-40, the direct adaptive method of Gupta and Kunnath [5]; and the modal pushover analysis advanced by Chopra and Goel [9]. The AMC procedure combines the response of individual modal pushover analyses to account for the influence of higher modes and incorporates the effects of changing modal properties during inelastic response through its adaptive feature. A unique aspect of the procedure is that the target displacement is estimated and updated dynamically during the analysis by incorporating energy based modal capacity curves with inelastic response spectra. Hence it eliminates the need to approximate the target displacement prior to commencing the pushover analysis. The basic steps of the methodology are summarized below though the reader is referred to the paper by Kalkan and Kunnath [14] for complete and comprehensive details:

1. Generate the capacity spectra for the selected ground motion in ADRS format (spectral acceleration $S_{a,n}(\mu, \zeta_n, \lambda_n)$ versus spectral displacement $S_{d,n}(\mu, \zeta_n, \lambda_n)$) for a series of predefined ductility levels. This step is required to calculate the energy based dynamic target displacement.

2. For the nth-mode considered, evaluate the lateral load pattern to be applied in the next step from $s_n^{(i)} = m\phi_n^{(i)}$ where (i) is the step number of the incremental adaptive pushover analysis and m is the mass matrix of the structure. This load distribution should be recomputed every time the system properties change due to inelastic action.
3. The capacity curve for each equivalent single degree-of-freedom (ESDOF) system is estimated using an energy based approach in which the increment in the energy based displacement of the ESDOF system, $\Delta D_n^{(i)}$ can be obtained as $\Delta D_n^{(i)} = \Delta E_n^{(i)}/V_{b,n}^{(i)}$ where $\Delta E_n^{(i)}$ is the increment of work done by lateral force pattern $s_n^{(i)}$ acting through the displacement increment, $\Delta d_n^{(i)}$, associated with a single step of the nth-mode pushover analysis. $V_{b,n}^{(i)}$ is the base shear at the ith step. The spectral displacement, $S_{d,n}^{(i)}$ (i.e., abscissa of the ESDOF capacity curve) at any step of nth-mode pushover analysis is obtained by the summation of $\Delta D_n^{(i)}$. The ordinate of the ESDOF capacity curve is computed in the usual manner as follows: $S_{a,n}^{(i)} = V_{b,n}/(\alpha_n^{(i)} W)$ where $\alpha_n^{(i)}$ is the modal mass coefficient computed at the ith step of the nth-mode pushover analysis.
4. Calculate the approximate global system ductility ($\mu_n^{(i)} = S_{d,n}^{(i)}/S_{d,n}^{(\text{yield})}$) if the response is found to be inelastic for each modal pushover analysis. The post-yield stiffness ratio ($\lambda_n^{(i)}$) can be approximated using a bilinear representation (see Kalkan and Kunnath [14] for details).
5. Plot $S_{a,n}^{(i)}$ versus $S_{d,n}^{(i)}$ together with the inelastic demand spectra (from Step 1) at different ductility levels. The dynamic target point, D_n^{ip} for the nth-mode pushover analysis is the intersection of the ESDOF modal capacity curve with the inelastic demand spectrum (i.e., $S_{a,n}(\mu, \zeta_n, \lambda_n)$ versus $S_{d,n}(\mu, \zeta_n, \lambda_n)$) corresponding to the global system ductility (μ).
6. Extract the desired values of response parameters ($r_n^{(ip)}$) at the ipth step of the nth-mode pushover analysis.

Repeat Steps 1–7 for as many modes as necessary for the system under consideration. The first few modes are typically adequate for most low to medium rise buildings. The total response is determined by combining the peak modal responses in an appropriate combination scheme (such as SRSS or CQC).

3. Structural systems, analytical models and ground motions

Existing 6 and 13 story steel moment frame buildings and 7 and 20 story RC moment frame buildings were used in the evaluation of the different NSP methods. All buildings were instrumented by the CSMIP (California Strong Motion Instrumentation Program), thus data from actual earthquake responses were used in the calibration of the mathematical models. Details of the structural systems and the calibration studies can be found in Kunnath et al. [15].

The 6-story steel building has a footprint of 36.6 m by 36.6 m with 6 bays in each lateral direction and a total height of 25.3 m while the plan dimensions of the 13-story building are 48.8 m by 48.8 m with 5 bays in each direction and an elevation of 57.5 m. The primary lateral load resisting system for both these buildings is a moment frame around the perimeter of the building. Interior frames are designed to carry only gravity loads. In each case, only a typical perimeter frame is considered in the evaluation.

The 7-story RC building is 20.03 m in elevation and has a rectangular plan with dimensions of 45.72 m × 18.6 m. The lateral load is resisted by four perimeter spandrel beam–column frames. The moment frames in the longitudinal direction consist of eight bays at 5.7 m. In the short direction, the two outer bays are 6.12 m and the interior bay measures 6.35 m. The interior frames comprise of 45.7 cm square columns and two way flat slabs. Finally, the 20-story RC building measures 60.7 m × 19.1 m in the longitudinal and transverse directions, respectively. The primary lateral force resisting system consists of moment-resisting frames with strong shear walls in the basement only. A typical frame in the longitudinal direction was considered in the analysis of each RC building.

3.1. Analytical model development

Analytical models were created using the open source finite element platform, OpenSees [16]. Two-dimensional models of a single frame were developed for each building. A force-based nonlinear beam–column element (utilizing a layered fiber section) is used to model all components of the frame models. Steel is modeled using a bilinear stress–strain curve with 2% post-yield hardening while the Kent-Park concrete model in OpenSees is used to model the concrete section. Confined properties were generated using the well-known and widely-used Mander's confinement model. Plastic rotation in OpenSees is defined as the maximum absolute total rotation minus the yield or recoverable rotation. To gain a better understanding of the development and implementation of nonlinear models in time-history analysis, the reader is referred to the textbook by Cheng [17]. Centerline dimensions were used in the element modeling, the composite action of floor slabs was not considered, and the columns were assumed to be fixed at the base level. For the time-history evaluations, masses were applied to frame models based on the floor tributary area and distributed proportionally to the floor nodes. The simulation models were calibrated to the measured response data so as to gain confidence in the analytical results of the comparative study.

3.2. Ground motion ensemble

In order to consider ground motions with diverse characteristics, ordinary far-fault records and near-fault ground motions having forward directivity and fling effects were used. A total of thirty records as indicated in Table 1 were compiled for the NTH analyses. The selection of near-fault records has two important features. First, these motions have significant PGV than ordinary far-fault records. Second, near-fault records exhibit intense coherent long period velocity pulses due to

Table 1
Details of ground motion ensemble

No	Year	Earthquake	M_W	Mech.[a]	Recording station	Dist. (km)[b]	Site Class[c]	Data Source[d]	Comp.	PGA (g)	PGV (cm/s)
Near-fault ground motions with forward directivity											
1	1979	Imperial-Valley	6.5	SS	EC Meloland Overpass	3.1	D	1	270	0.30	90.5
2	1984	Morgan Hill	6.1	SS	Coyote Lake Dam	1.5	B	2	285	1.16	80.3
3	1989	Loma Prieta	7.0	OB	Saratoga Aloha Ave.	4.1	D	2	090	0.32	44.8
4	1989	Loma Prieta	7.0	OB	Lexington Dam	6.3	C	2	090	0.41	94.3
5	1992	Erzincan	6.7	SS	Erzincan	2.0	C	1	EW	0.50	64.3
6	1992	Cape Mendocino	7.1	TH	Petrolia, General Store	15.9	C	1	090	0.66	90.2
7	1994	Northridge	6.7	TH	Rinaldi Receiver Stn.	8.6	D	2	S49W	0.84	174.8
8	1994	Northridge	6.7	TH	Jensen Filtration Plant	6.2	D	1	292	0.59	99.2
9	1995	Kobe	6.9	SS	JMA	0.6	C	1	000	0.82	81.6
10	1995	Kobe	6.9	SS	Takatori	4.3	D	1	090	0.62	120.8
Near-fault ground motions with fling											
1	1999	Kocaeli	7.4	SS	Sakarya	3.20	C	3	EW	0.41	82.1
2	1999	Chi-Chi	7.6	TH	TCU068	3.01	D	4	EW	0.50	277.6
3	1999	Chi-Chi	7.6	TH	TCU072	7.87	D	4	EW	0.46	83.6
4	1999	Chi-Chi	7.6	TH	TCU074	13.8	D	4	EW	0.59	68.9
5	1999	Chi-Chi	7.6	TH	TCU084	11.4	C	4	NS	0.42	42.6
6	1999	Chi-Chi	7.6	TH	TCU129	2.2	D	4	EW	0.98	66.9
7	1999	Chi-Chi	7.6	TH	TCU082	4.5	D	4	EW	0.22	50.5
8	1999	Chi-Chi	7.6	TH	TCU078	8.3	D	4	EW	0.43	41.9
9	1999	Chi-Chi	7.6	TH	TCU076	3.2	D	4	NS	0.41	61.8
10	1999	Chi-Chi	7.6	TH	TCU079	10.95	D	4	EW	0.57	68.1
Far-fault ground motions											
1	1952	Kern county	7.5	TH/REV	Taft	36.2	D	1	111	0.18	17.5
2	1989	Loma Prieta	7.0	OB	Cliff House	68.5	D	1	090	0.11	19.8
3	1992	Big Bear	6.4	SS	Desert Hot Spr. (New Fire Stn.)	40.1	D	2	090	0.23	19.1
4	1994	Northridge	6.7	TH	Moorpark (Ventura Fire Stn.)	26.4	D	2	180	0.29	21.0
8	1994	Northridge	6.7	TH	Saturn Street School	26.9	D	2	S70E	0.43	43.5
3	1971	San Fernando	6.6	TH	Castaic, Old Ridge Route	23.5	B	1	291	0.27	25.9
7	1971	Landers	7.3	SS	Boron Fire Stn.	99.3	D	1	000	0.12	13.0
8	1989	Loma Prieta	7.0	OB	Presidio	67.4	D	1	090	0.19	32.4
9	1994	Northridge	6.7	TH	Terminal Island Fire Stn. 111	57.5	D	1	330	0.19	12.1
10	1994	Northridge	6.7	TH	Montebello	44.2	D	1	206	0.18	9.4

[a] Faulting mechanism = TH: Thrust; REV: Reverse; SS: Strike-slip; OB: Oblique.
[b] Closest distance to fault.
[c] NEHRP Site Class = B for V_S (Shear-wave velocity) = 760–1500 m/s; C for V_S = 360–760 m/s; D for V_S = 180 to 360 m/s.
[d] Data source = 1: PEER (http://peer.berkeley. edu/smcat); 2: Cosmos (http://db.cosmos-eq.org) 3: ERD (http://angora.deprem.gov.tr/); 4: http://scman.cwb.gov.tw/eqv5/special/19990921/pgadata-asci0704.htm.

directivity effects. As opposed to near-fault forward directivity records generally producing two sided velocity pulses, near-fault fling types of records are generally characterized with a single sided velocity peak and that manifests itself as a large static offset at the end of the displacement time-history. This static offset is the indication of tectonic deformation on the rupture plane. To get the true tectonic deformation, raw fling records should be processed by avoiding conventional filtering techniques (i.e., band-pass filters). Accordingly, raw fling records in the dataset were corrected by applying baseline correction only following the removal of pre-event mean (see Kalkan and Kunnath [18] for details of the correction process).

3.3. Ground motion scaling and target displacement evaluation

In order to facilitate a rational basis for comparison of the different methodologies, the ground motion records given in Table 1 were scaled so that a peak roof drift ratio of 1.5% was achieved for the two steel buildings and the 7-story RC building while a roof drift of 1% was obtained for the 20-story RC building. Fig. 1 displays the elastic mean pseudo-acceleration spectra (five percent damped) of the building-specific scaled records. Also marked on this figure with vertical lines are the first three elastic fundamental periods of the buildings.

The target displacements used for the FEMA-356 and UBPA procedures are the predetermined peak roof displacements for each building. For the MMPA, this target displacement was used to calculate the first mode contribution. For the second and third mode contributions, the mean spectra computed for each building and ground motion set were used together with the elastic modal periods to determine the peak roof displacement levels. For AMC, the target point for the first mode was constrained to the predetermined peak roof drift, and the target point for the higher modes (i.e., 2nd and 3rd) were

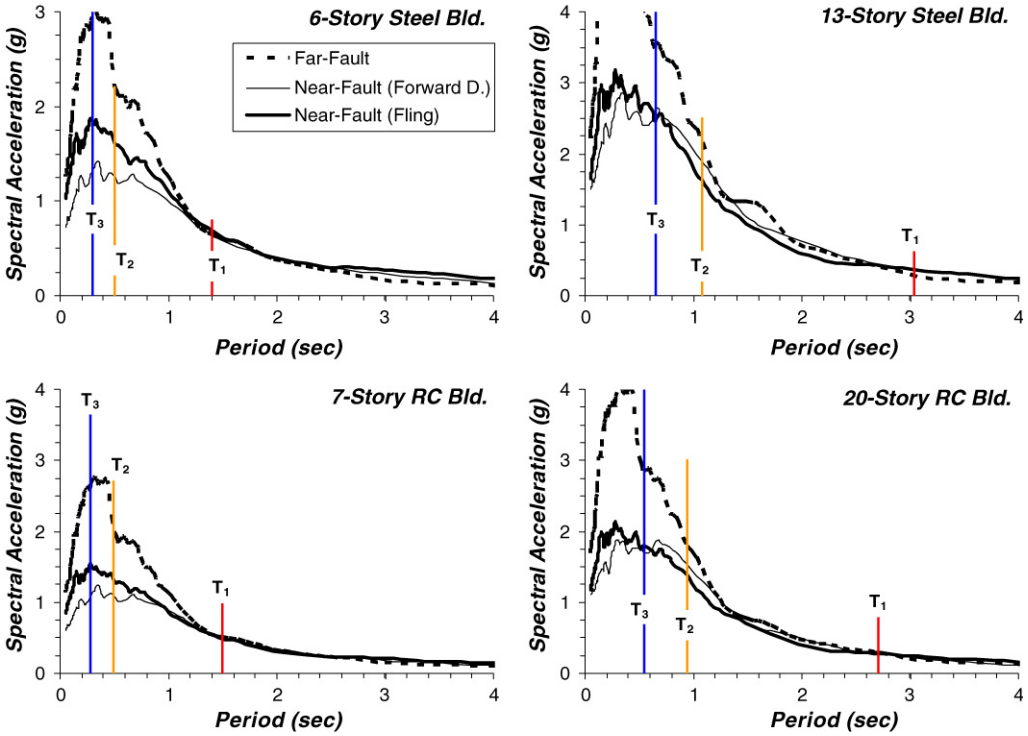

Fig. 1. Mean pseudo-acceleration spectra of building-specific scaled ground motions.

computed dynamically during the pushover analyses using the mean inelastic spectra of the records.

4. Evaluation of nonlinear static procedures

The FEMA-356, MMPA, UBPA and AMC nonlinear static procedures are evaluated by comparing the computed roof drift ratio (maximum roof displacement normalized by building height), interstory drift ratio (relative drift between two consecutive stories normalized by story height) and member plastic rotations to nonlinear time-history results. Since the time-history results are based on a set of ten simulations per record set, both the mean and the dispersion (standard deviation) about the mean value are presented in the plots.

4.1. Peak displacement profiles

Figs. 2 and 3 show the mean and standard deviations (i.e., 16 and 84 percentile) of the peak displacement profile estimated by NTH analyses and predictions by FEMA-356, UBPA, MMPA and AMC procedures for each building sorted by type of record. The peak deformed shape along the heights of the buildings show that FEMA-356 pushover envelope consistently overestimates the peak story displacements in the low and intermediate story levels for all buildings and ground motions types investigated, while UBPA underestimates the displacements at almost all levels with the exception of the upper stories. The AMC and MMPA procedures both result in similar estimates and generally yield better estimates of the peak displacement profile particularly for the 13-story steel and 7-story RC buildings. It is interesting that story displacement demands from nonlinear static methods (with the exception of UBPA) are always conservative. Comparing the time-history responses for the different ground motions indicates that far-fault records generally produce more variability in the demands than near-fault records. Only the 20-story RC building showed greater variability in the displacement demands for near-fault records.

4.2. Interstory drift ratio profiles

In Figs. 4 and 5, the interstory drift ratio profiles obtained with NSPs are compared to NTH estimates. For the entire set of analyzed buildings, significant higher mode contributions are evident resulting in the migration of dynamic drifts from the lower to the upper stories. The FEMA-356 methodology grossly underestimates the drifts in upper stories and overestimates them in lower stories, except the 13-story building, in which only the lower level demands were captured adequately. Conversely, the UBPA always underestimates the drifts at the lower levels and overestimates them at the upper story levels. MMPA yields better estimates of drift demands compared to FEMA-356 and UBPA. However, in all cases, upper level demands were underestimated by MMPA, with the exception of the 13-story building, where MMPA overestimates the upper level drifts. On the other hand, AMC is shown to predict the drift profiles for all four buildings with relatively better accuracy. The AMC procedure slightly overestimates or underestimates the drift in some cases but captures the overall effects of higher mode contributions more consistently for both far-fault and near-fault records.

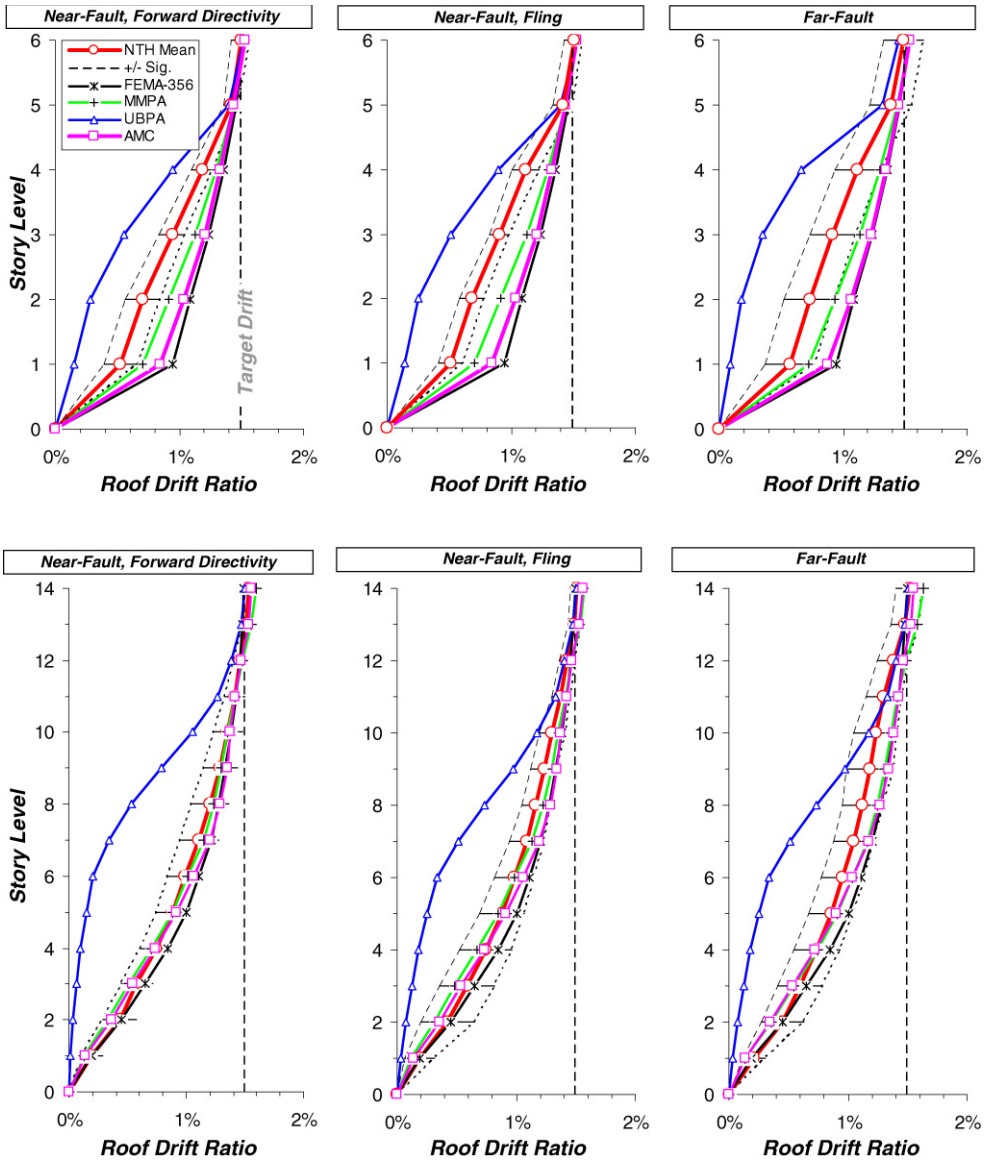

Fig. 2. Predicted peak displacement demands by NSPs compared to NTH analyses for steel buildings.

4.3. Member plastic rotation profiles

Since each earthquake record induces different demand patterns, local demand estimates at the component level are evaluated only for a specific record in each data set (near fault with directivity, near fault with fling and far-fault record). Figs. 6 and 7 show the results of computed member plastic rotations at beams and columns determined by NTH and are compared to NSP estimates for the 6-story steel and 7-story RC buildings, respectively. Only the AMC and MMPA procedures are included here since the comparisons presented previously have demonstrated the limitations of the FEMA and UBPA methods.

It is seen that MMPA fails to identify column yielding in the 5th level of the 6-story steel frame but does a good job at the first story level. The AMC procedure is able to identify plastic hinging at both the first and fifth levels. MMPA provides an improved prediction for the 7-story RC frame by identifying yielding in the fourth story: however it is unable to capture the inelastic demands at the other levels. AMC predictions are consistent with NTH patterns though the demands are slightly overestimated for the near-fault record with directivity effects. The plastic rotation estimates in MMPA are produced essentially by the first mode pushover analysis while higher modes contributions remain elastic as per the procedure. Accordingly, MMPA generally provides better estimates of plastic rotations at the first and lower story levels.

5. Higher mode contributions to seismic demands

Higher mode effects on seismic demand are strongly dependent on both the characteristics of the ground motion and the properties of the structural system. While the former is an independent input parameter, the dynamic properties of the structural system are significantly affected by the frequency content of the ground motion. With repeated changes in

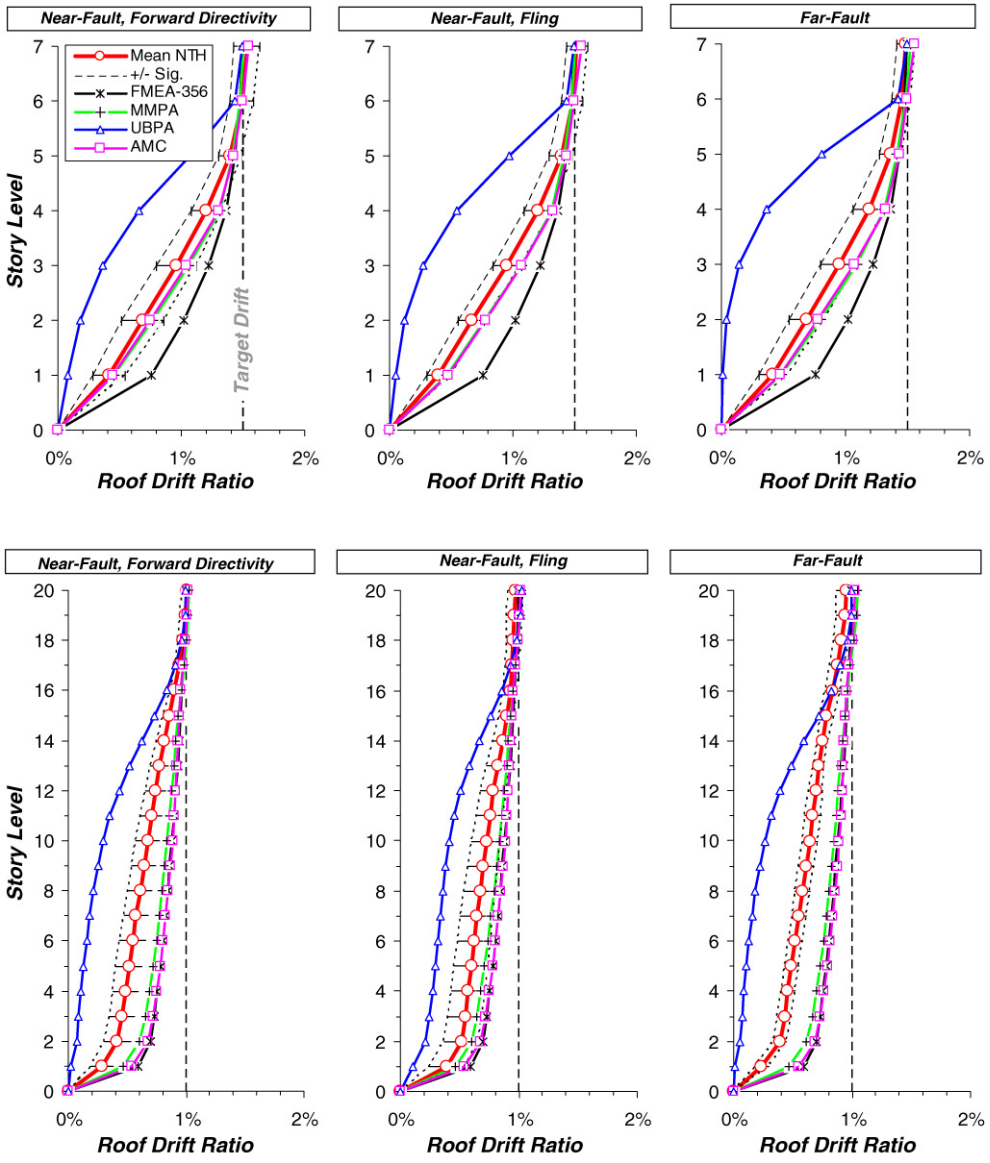

Fig. 3. Predicted peak displacement demands by NSPs compared to NTH analyses for RC buildings.

system stiffness, modal attributes also experience progressive modifications. Fig. 8 demonstrates how modal periods and modal participation factors are altered during the dynamic response of the 6-story building when subjected to JMA near-fault record. The peak interstory drift profile (Fig. 8(d)) shows that the peak drift is occurring at the fifth story level, a clear indication of higher mode effects. It is instructive to note that the peaks of modal periods (associated with yielding and inelastic behavior) are associated with the peaks of the modal participation factors, and they strongly correlate to the time steps at which the story peak demands occur (follow the vertical lines in Fig. 8). Another important observation is that the second and third mode modal participation factors are in-phase but both these modes are out-of-phase with respect to the first mode participation factor. That implies that the peak deformation associated with the first mode (at the first story in this case) is not coupled with higher mode contributions.

Fig. 9 demonstrates other important features of structural behavior by examining snapshots of the time-history response of the same building. Shown in this figure are the inertia forces computed by multiplying story mass and story acceleration at the time instances when the peak interstory drift demands at each story level are observed. Notably, peak demands at each story occur at different time instances with significantly different inertia force patterns. Consideration of the vertical distribution of inertia forces is crucial for static procedures and such variations can only be accommodated by considering changes in the modal attributes as the system moves from the elastic to inelastic state.

Fig. 10 shows how the mode shapes vary continuously during the response history. Mode shapes shown in this figure are from snapshots at critical time instants when the peak interstory drift occurs at each story level. In fact, these changes are also reflected in the instantaneous inertia forces described in the previous paragraph. At the time when the first story

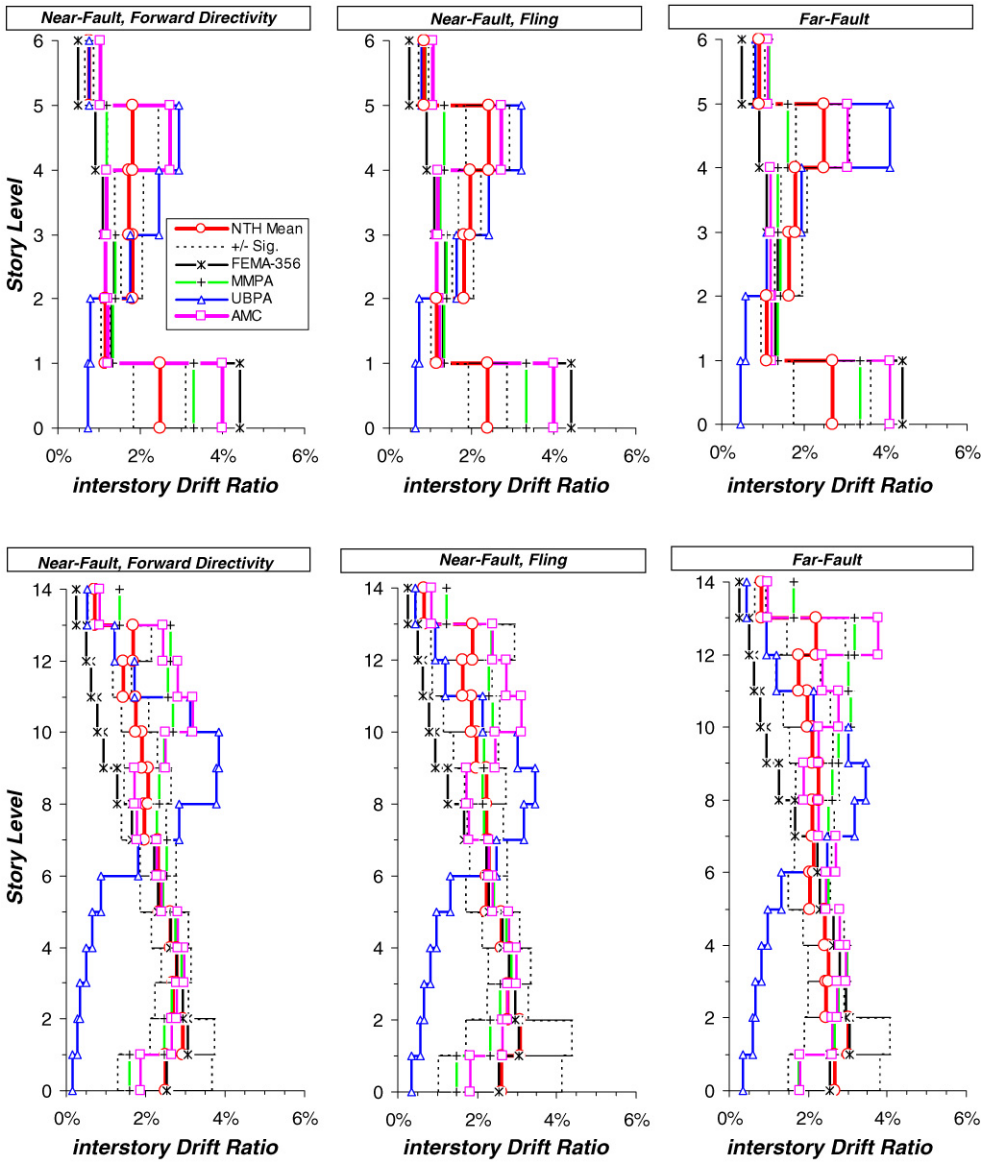

Fig. 4. Predicted peak interstory drift demands by NSPs compared to NTH analyses for steel buildings.

experiences its peak demand, the first mode shape resembles the FEMA invariant uniform load distribution. At the time step when the fifth story peak drift is recorded, the first mode shape has significantly deviated from its original elastic form forcing the upper story levels to deform further rather than the lower levels. The significant contribution of the second mode to the relative drift between the fourth and fifth level is evident as the system moves from the elastic to inelastic phase. Similarly, the third mode is seen to influence the drift mostly at the mid-levels though the relative difference is not significant. These observations once again highlight the importance of considering mode shapes at different stiffness states of the system.

6. Conclusions

This paper critically examines the ability of four different types of nonlinear static procedures to predict seismic demands in a set of existing buildings. Each building is subjected to 30 ground motions having different characteristics. The resultant mean and standard deviations served as benchmark responses against which the NSPs were compared. A systematic evaluation of the predicted demands (such as peak displacement profile, interstory drifts and member plastic rotations) by the different NSPs forms the basis for the following conclusions:

1. The FEMA-356 method (wherein the envelope of two response measures were considered) provides inadequate predictions of peak interstory drift and peak member plastic rotations at the upper story levels when higher mode contributions are significant.
2. UBPA estimates were the poorest by far, being unable to reasonably predict even the peak displacement profile. It led to significant underestimation of story drift demands and member rotations at the lower levels and to their overestimation at the upper stories.

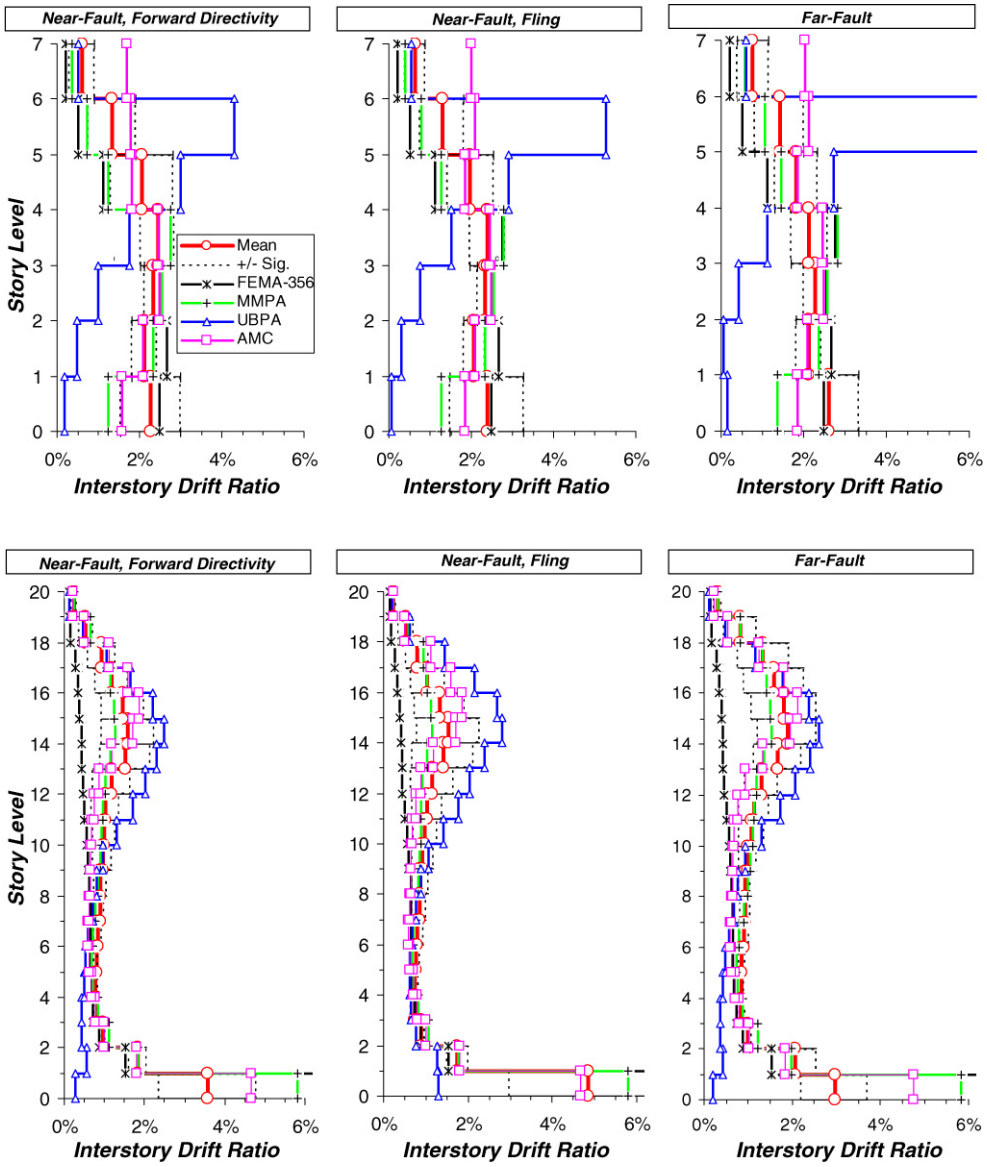

Fig. 5. Predicted peak interstory drift demands by NSPs compared to NTH analyses for RC buildings.

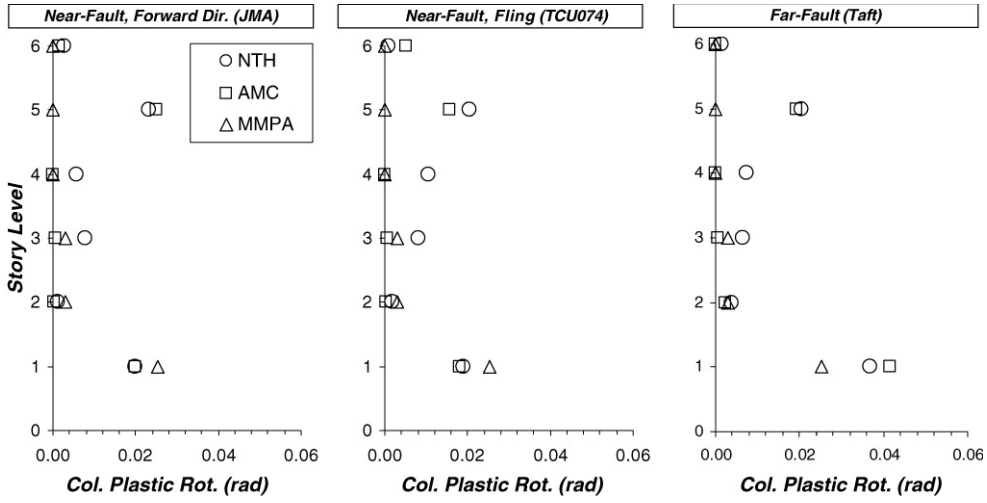

Fig. 6. Predicted maximum column plastic rotations by AMC and MMPA compared to NTH analyses for 6-story steel building subjected to (scaled) JMA, TCU074 and Taft records.

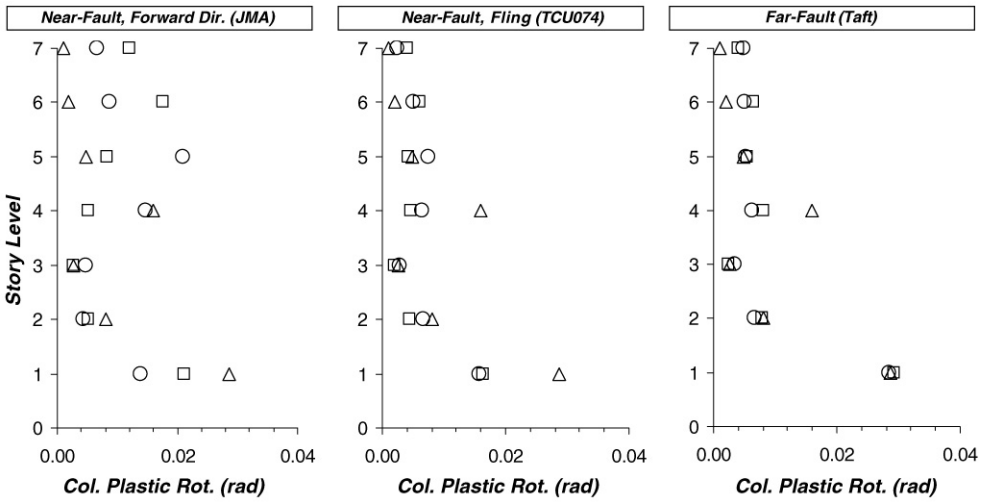

Fig. 7. Predicted maximum column plastic rotations by AMC and MMPA compared to NTH analyses for 7-story RC building subjected to (scaled) JMA, TCU074 and Taft records.

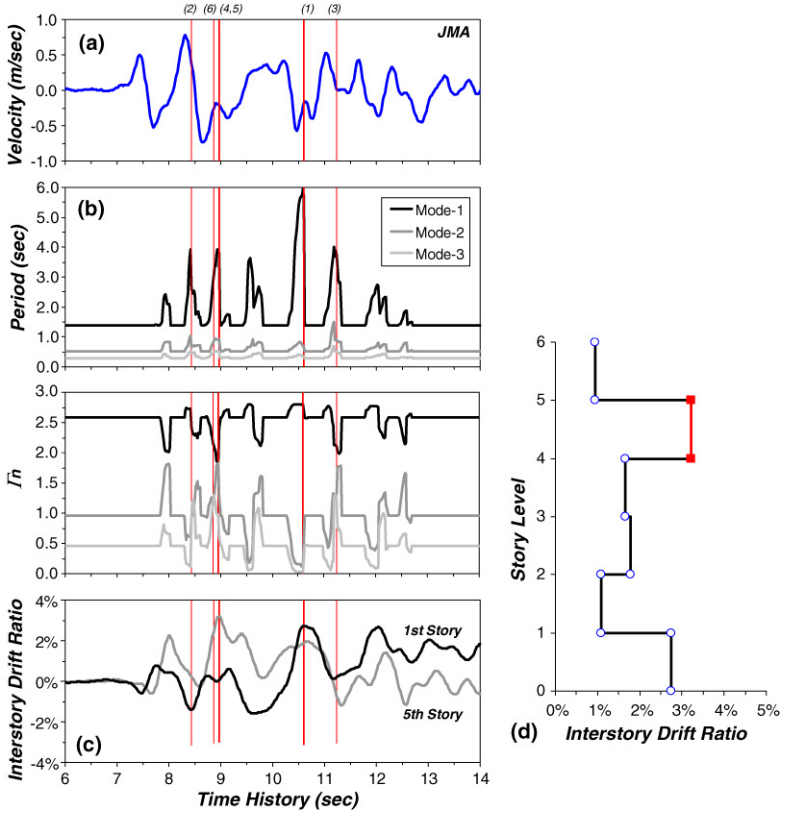

Fig. 8. (a) Velocity–time series of JMA motion; (b) variation of 6-story building modal periods and nth-mode participation factor (Γ_n); (c) interstory drift history; (d) peak interstory drift profile (*note that the number in parentheses at the top indicates the specific story that has the peak interstory drift at the time instant indicated by vertical line*).

3. Compared to FEMA-356 and UBPA procedures, MMPA provides story drift estimates that are generally much closer to the mean NTH estimates. However, since the method ignores the inelastic contribution of higher modes, it is unable to reasonably predict plastic rotation demands in the upper stories.
4. It was also shown that NSPs based on invariant load vectors using elastic modal properties cannot capture the changes to the dynamic modes resulting from inelastic action. The inertia load distribution, which is well correlated to story deformations, progressively changes following the variation of the modal periods and modal shapes during inelastic response. Consequently, the variation of inertial forces must be considered in static procedures that attempt to reproduce inelastic dynamic response. This can only be achieved using adaptive load vectors.

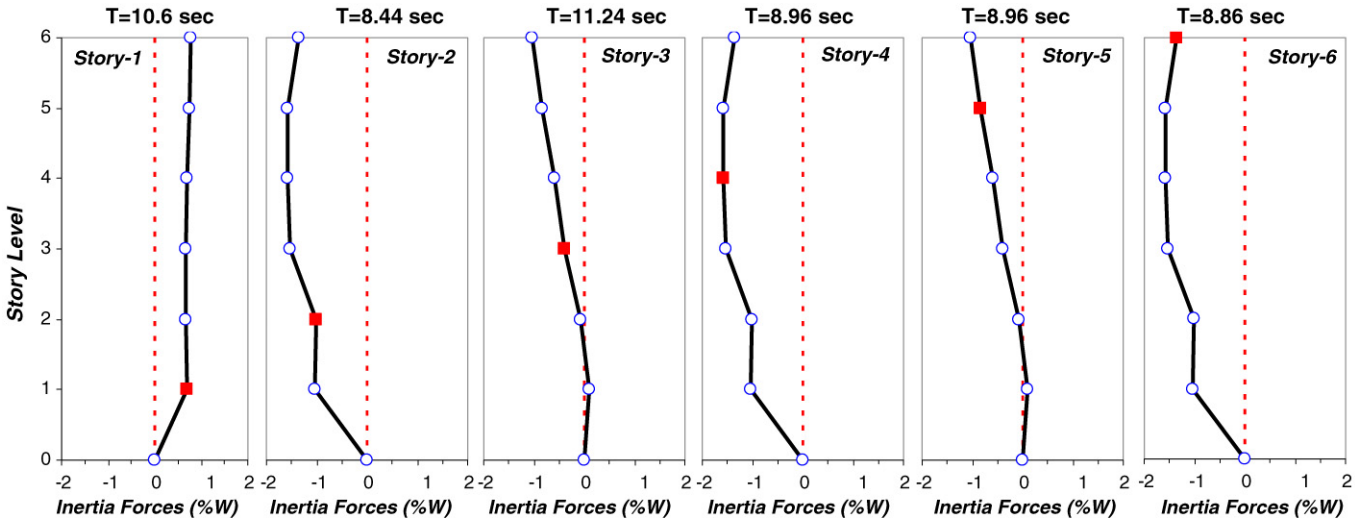

Fig. 9. Instantaneous inertia profiles when the story maxima take place (*6-story building subjected to JMA motion, 'T' indicates the time instance in the time-history, filled square marker indicates the critical story at the specific time instant, T*).

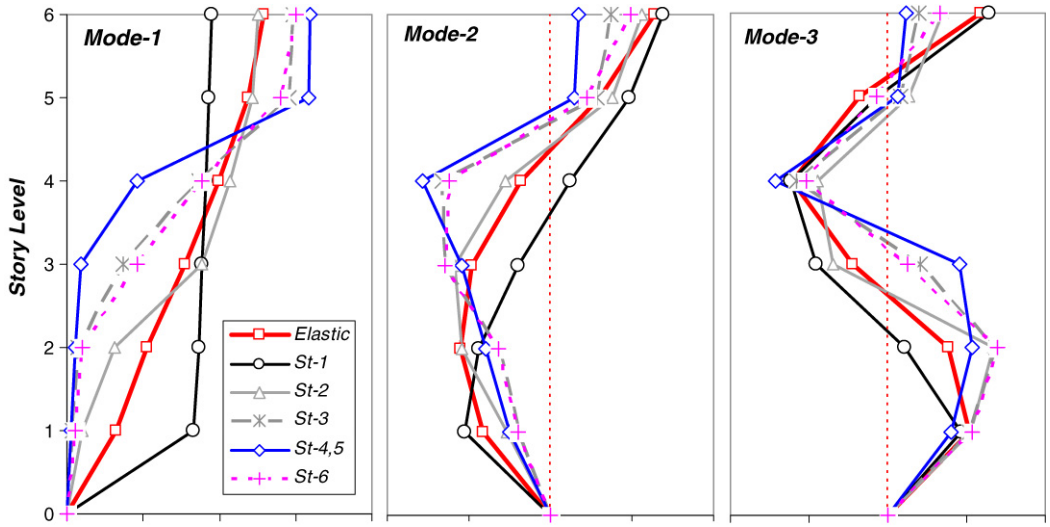

Fig. 10. Instantaneous modal shapes at the time instances when the story maxima take place (*6-story building subjected to JMA motion; 'St' in legend indicates story level*).

5. The recently developed AMC procedure which integrates the inherent advantages of the capacity spectrum method, modal combination and adaptive loading scheme provided the best overall comparison with NTH results. In general, the method was able to reproduce the essential response features providing a reasonable measure of the likely contribution of higher modes in all phases of the response.

Acknowledgments

Funding for this study provided by the National Science Foundation under Grant CMS-0296210, as part of the US–Japan Cooperative Program on Urban Earthquake Disaster Mitigation, is gratefully acknowledged. Any opinions, findings, and conclusions or recommendations expressed in this material are those of the authors, and do not necessarily reflect the views of the National Science Foundation.

References

[1] The Ministry of Land, Infrastructure and Transport. Design example and commentary for the calculation of response and limit strength 2001 [in Japanese].

[2] CEN. Eurocode 8 – Design of Structures for Earthquake Resistance, Part -1. European Standard prEN 1998-1. Draft no. 4. Brussels: European Committee for Standardization; December 2001.

[3] Applied Technology Council (ATC). Seismic evaluation and retrofit of concrete buildings. Volumes 1 and 2. Report no. ATC-40, Redwood City (CA), 1996.

[4] American Society of Civil Engineers (ASCE). Prestandard and commentary for the seismic rehabilitation of buildings. FEMA-356. Washington DC; 2000.

[5] Gupta B, Kunnath SK. Adaptive spectra-based pushover procedure for seismic evaluation of structures. Earthquake Spectra 2000;16(2):367–91.

[6] Kunnath SK, Kalkan E. Evaluation of seismic deformation demands using nonlinear procedures in multistory steel and concrete moment frames. ISET, Journal of Earthquake Technology 2004;41(1):159–82.

[7] Kalkan E, Kunnath SK. Method of modal combinations for pushover analysis of buildings. In: Proc. of the 13th world conference on earthquake engineering, Paper no. 2713. 2004.
[8] Goel RK, Chopra AK. Evaluation of modal and FEMA pushover analyses: SAC buildings. Earthquake Spectra 2004;20(1):225–54.
[9] Chopra AK, Goel RK. A modal pushover analysis procedure for estimating seismic demands for buildings. Earthquake Engineering and Structural Dynamics 2002;31:561–82.
[10] Chopra AK, Goel RK, Chintanapakdee C. Evaluation of a modified MPA procedure assuming higher modes as elastic to estimate seismic demands. Earthquake Spectra 2004;20(3):757–78.
[11] Jan TS, Liu MW, Kao YC. An upper-bound pushover analysis procedure for estimating seismic demands of high-rise buildings. Engineering Structures 2004;26:117–28.
[12] Elnashai AS. Advanced inelastic (pushover) analysis for seismic design and assessment. In: The G. Penelis Symposium. 2000.
[13] Antonio S, Pinho R. Development and verification of a displacement-based adaptive pushover procedure. Journal of Earthquake Engineering 2004;8(5):643–61.
[14] Kalkan E, Kunnath SK. Adaptive modal combination procedure for nonlinear static analysis of building structures. ASCE Journal of Structural Engineering 2006 [in press].
[15] Kunnath SK, Nghiem Q, El-Tawil S. Modeling and response prediction in performance-based seismic evaluation: Case studies of instrumented steel moment-frame buildings. Earthquake Spectra 2004;20(3):883–915.
[16] OpenSees 2005. Open system for earthquake engineering simulation. Available online: http://opensees.berkeley.edu.
[17] Cheng FY. Matrix analysis of structural dynamics — applications and earthquake engineering. Marcel Dekker; 2001. p. 997.
[18] Kalkan E, Kunnath SK. Effects of fling-step and forward-rupture directivity on the seismic response of buildings. Earthquake Spectra 2006; 22(2):367–90.